Chemistry & Biology
Article

A General Framework for Inhibitor Resistance in Protein Kinases

Deborah Balzano,[1,3] Stefano Santaguida,[1] Andrea Musacchio,[1,2,*] and Fabrizio Villa[1,*]
[1]Department of Experimental Oncology, European Institute of Oncology, Via Adamello 16, 20139 Milan, Italy
[2]Max Planck Institute of Molecular Physiology, Otto-Hahn-Strasse 11, 44227 Dortmund, Germany
[3]Present address: Structural Biology and Biocomputing Programme, Spanish National Cancer Research Centre (CNIO), c/Melchor Fdez. Almagro 3, 28029 Madrid, Spain
*Correspondence: andrea.musacchio@mpi-dortmund.mpg.de (A.M.), fabrizio.villa@ifom-ieo-campus.it (F.V.)
DOI 10.1016/j.chembiol.2011.04.013

SUMMARY

Protein kinases control virtually every aspect of normal and pathological cell physiology and are considered ideal targets for drug discovery. Most kinase inhibitors target the ATP binding site and interact with residue of a hinge loop connecting the small and large lobes of the kinase scaffold. Resistance to kinase inhibitors emerges during clinical treatment or as a result of in vitro selection approaches. Mutations conferring resistance to ATP site inhibitors often affect residues that line the ATP binding site and therefore contribute to selective inhibitor binding. Here, we show that mutations at two specific positions in the hinge loop, distinct from the previously characterized "gatekeeper," have general adverse effects on inhibitor sensitivity in six distantly related kinases, usually without consequences on kinase activity. Our results uncover a unifying mechanism of inhibitor resistance of protein kinases that might have widespread significance for drug target validation and clinical practice.

INTRODUCTION

In eukaryotes, protein kinases are implicated in nearly any signaling pathway under both physiological and abnormal conditions (Cohen, 2002). In human cancer, deregulation of protein kinase activity often correlates with disease progression. Accordingly, various members of the protein kinase family are recognized as targets for anticancer therapy, and small-molecule kinase inhibitors represent an important class of anticancer agents (Bikker et al., 2009; Karaman et al., 2008; Knight and Shokat, 2005; Zhang et al., 2009). The small-molecule inhibitor imatinib (also known as Gleevec), for instance, has revolutionized the treatment of chronic myeloid leukemia (CML) (Capdeville et al., 2002). In CML patients, a chromosomal translocation leads to the creation of the BCR-ABL gene. c-Abl is a tyrosine kinase whose activity in normal cells is tightly regulated. Within the Bcr-Abl fusion protein, Abl activity becomes constitutive (Suryanarayan et al., 1991; Wong and Witte, 2004).

Imatinib is a potent and selective active-site inhibitor of Bcr-Abl. Its remarkable clinical efficacy, however, is counteracted by the emergence of clinical resistance (Gorre et al., 2001). The most common mechanism for imatinib resistance is the emergence of mutations in the Abl kinase domain (Krishnamurty and Maly, 2010). Over 50 different point mutations in the c-Abl kinase domain have been detected in imatinib-resistant CML patients (Melo and Chuah, 2007). Several mutations affect residues in the vicinity of the ATP binding site, such as Y253 and E255 in the phosphate-binding loop (P loop) (Figure 1A). Additional hot spots of mutations are in the hinge loop, which connects the small and large lobes and provides a scaffold for adenine binding. $T315^{Abl}$, also known as the gatekeeper residue (Branford et al., 2002), is a prominent hot spot of mutation in the hinge loop (Figure 1A). Gatekeeper mutations disrupt the inhibitor-binding interface without grossly affecting the catalytic properties of the enzyme, and therefore satisfy the tumor cells' addiction to Abl activity while rendering them resistant to imatinib (Gorre et al., 2001). Remarkably, mutations of the gatekeeper residues of the ALK tyrosine kinase confer resistance to the small-molecule inhibitor crizotinib in EML4-ALK tumor cells (Choi et al., 2010). Similarly, EGFR kinase mutations at the gatekeeper confer resistance to erlotinib and gefitinib in lung tumors (Kobayashi et al., 2005; Pao et al., 2005).

Imatinib is a so-called type II inhibitor. Type II inhibitors induce a distinct conformation of the activation segment. Besides occupying the ATP site, they exploit a hydrophobic pocket created by this rearrangement (Schindler et al., 2000). Type I inhibitors, on the other hand, bind exclusively in and around the ATP binding site (Liu and Gray, 2006; Okram et al., 2006). Type II inhibitors are generally sensitive to mutations in the gatekeeper residue, whereas type I inhibitors are usually, although not universally, less sensitive to gatekeeper mutations.

Indeed, type I inhibitors VX-680 and dasatinib target the gatekeeper and other imatinib-resistant mutants of Abl (Carter et al., 2005; Shah et al., 2004). Nevertheless, certain imatinib-resistant hinge loop mutants of Abl, most prominently F317L, are also resistant to dasatinib (Aguilera and Tsimberidou, 2009; Soverini et al., 2006). Interestingly, an in vitro screen aiming to identify mutations conferring resistance to ZM447439, an Aurora B inhibitor, converged on $Y156^{AurB}$, corresponding to $F317^{Abl}$ (Girdler et al., 2008) (Figures 1A and 1B). Another position in the hinge loop, $G321^{Abl}$, is found mutated in cases of clinical resistance to imatinib (Melo and Chuah, 2007). Mutations at the equivalent position in Aurora B, $G160^{AurB}$, also confer resistance to

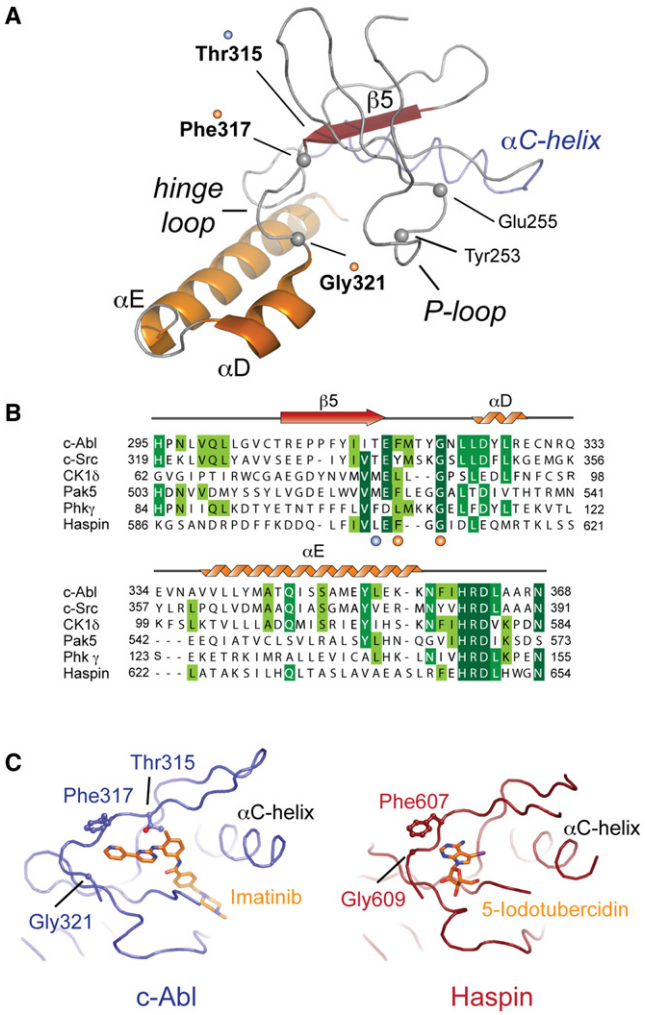

Figure 1. Structural Basis of Inhibitor Resistance

(A) Ribbon representation of a portion of the c-Abl kinase domain including the small lobe and part of the helical array of the large lobe (pdb id: 2fo0). The position of inhibitor-resistant mutants discussed in the text is mapped onto the model.

(B) Multiple sequence alignment of the hinge region of kinases analyzed in this study. The positions of hinge loop residues mutated in this study and of the gatekeeper are highlighted with orange and blue spheres, respectively.

(C) Ribbon representation of the active site and hinge loop of Abl with bound imatinib (blue, pdb id: 2fo0) and of Haspin with bound 5-iodotubercidin (red, pdb id: 3iq7). Residues selected as candidates for this study are represented as sticks. Molecular models were rendered with pymol (www.pymol.org).

See also Figure S1.

ZM447439 and other type I inhibitors of Aurora B (Girdler et al., 2008).

These previous results suggest the interesting possibility that mutations affecting the hinge loop of protein kinases have the potential to confer inhibitor resistance independently from the specific active-site inhibitor used (i.e., whether type I or type II) and independently of the specific chemical scaffold. To test this idea systematically, we introduced individual amino acid substitutions into the hinge region of six distant protein kinases and determined the inhibitor sensitivity of the mutant kinases against structurally distinct inhibitors (Table 1; see Figure S1 available online). Here, we report the results of our efforts.

Table 1. Protein Kinases and Inhibitors Employed in This Study

Protein Kinase	Group	Family	PDB	Inhibitor
c-Abl	TK	Abl	2fo0	VX-680
				Imatinib
				Dasatinib
				Nilotinib
				Staurosporine
c-Src	TK	Src	1fmk	VX-680
				PP1
				Staurosporine
CK1δ	CK1	CK1	1cki	D4476
Haspin	Other	Haspin	2wb8	5-Iodotubercidin
Pak5	STE	STE20	2f57	Staurosporine
Phkγ	CAMK	PHK	1phk	Staurosporine

RESULTS

A Data Set of Distant Protein Kinases

To generate a sufficiently diverse data set, we selected six kinases belonging to different groups in the classification of the eukaryotic protein kinases (ePK) fold (Manning et al., 2002). The six kinases included (1) c-Abl [belonging to the tyrosine kinase (Hung et al., 2007) subgroup]; (2) c-Src (also in the TK group); (3) casein kinase 1 [CK1δ, belonging to the casein kinase (CK1) group]; (4) Pak5 [belonging to the homologs of yeast Sterile 7, Sterile 11, Sterile 20 (STE) group]; (5) phosphorylase kinase [Phkγ, belonging to the calcium/calmodulin-dependent protein kinase (CAMK) group]; and Haspin, which does not belong to a specific group and is usually classified as "other" or "atypical." Thus, the six kinases in our data set are phylogenetically distant. We did not include kinases of the group containing the PKA, PKG, and PKC families (AGC group) because of previous evidence that Aurora B, a member of this group, becomes resistant to several active-site inhibitors when mutated at the same positions (Girdler et al., 2008). Additional criteria for their selection are (1) that recombinant, active versions of the kinases can be produced relatively straightforwardly; (2) that the kinases are structurally characterized (see Table 1); and (3) that one or more public domain small-molecule inhibitors are available for each of them (Table 1; Figure S1).

A sequence alignment of the hinge loop of the six kinases is shown in Figure 1B. A light blue dot at the bottom of the alignment marks the "gatekeeper" residue. The red dots mark Phe317 and Gly321 of c-Abl, and homologous residues in the other five kinases in our data set (we will use Abl numbering to refer to these positions unless otherwise indicated). The Kinase Sequence Database (KSD; http://sequoia.ucsf.edu/ksd/) provides exhaustive sequence information on protein kinases. In kinase sequence alignment from the KSD, the gatekeeper residue is marked in red. The positions corresponding to $Phe317^{Abl}$ and $Gly321^{Abl}$ are found in most cases at positions +2 and +6 from the gatekeeper, respectively. In all six kinases in our data set, there is a glycine residue at the position equivalent to

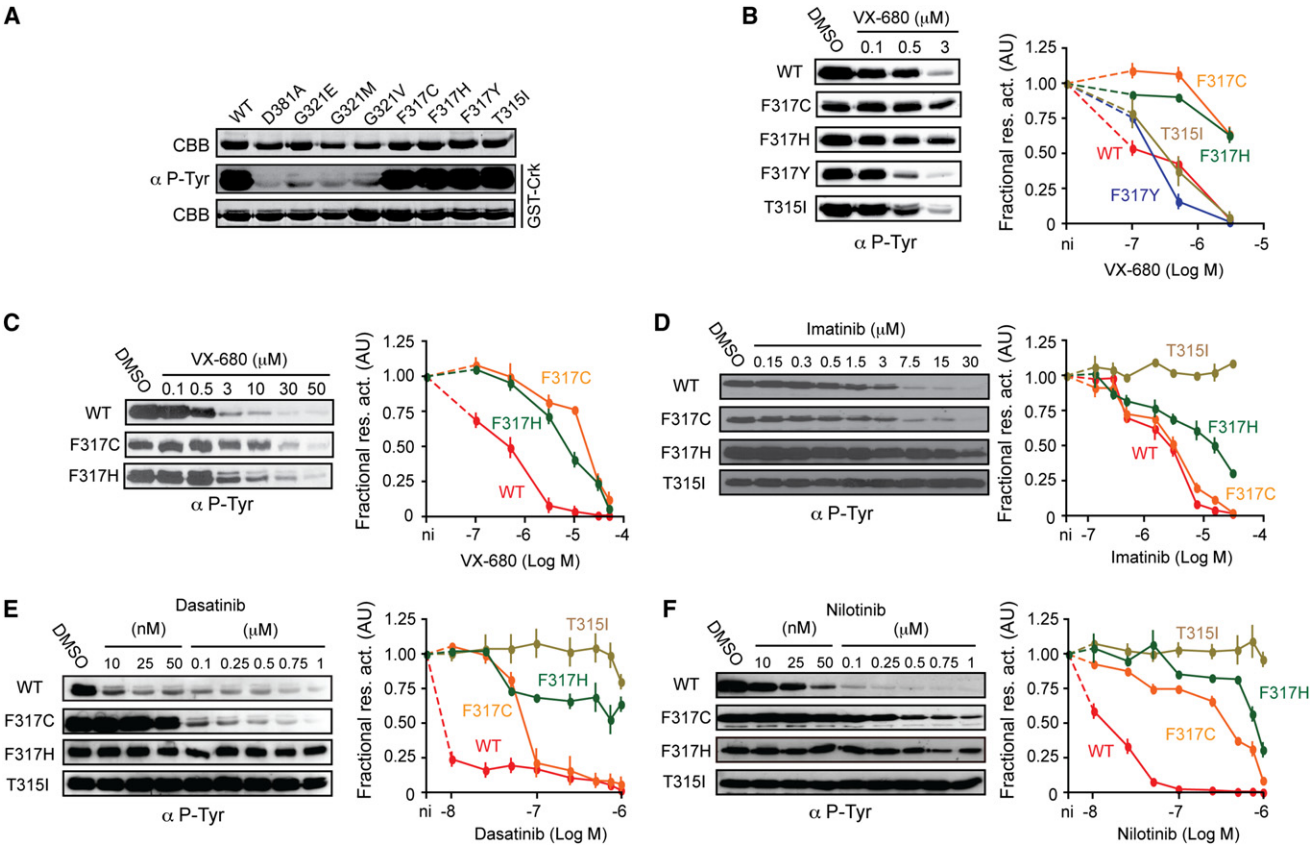

Figure 2. c-Abl VX-680-Resistant Mutants

(A) Activity test on wild-type c-Abl and the indicated mutants.

(B–F) Wild-type Abl and the indicated Abl mutants were tested in the presence of increasing concentrations of (B and C) VX-680, (D) imatinib, (E) dasatinib, and (F) nilotinib. Activity in the presence of DMSO solvent control (3% v/v) is also shown. Fractional residual activity (Fractional res. act.), from at least two independent experiments, expressed as mean and standard deviation [arbitrary unit (AU)] was then quantified and plotted against the inhibitors concentration. CBB: Coomassie brilliant blue, α P-Tyr: antibody recognizing phosphotyrosine residues. The condition marked as "ni" indicates absence of the inhibitor. Here and elsewhere in this work, this condition is assigned fractional activity of 1.0 as expected in the absence of inhibitors.

See also Figure S2.

Gly321^{Abl} (Figure 1B). As far as position Phe317^{Abl} is concerned, Pak5 and Haspin also have phenylalanine, Phkγ and CK1δ have leucine, and c-Src has tyrosine (Figure 1B). We mutated these two positions individually in each of the six kinases. The mode of inhibitor binding of two kinases in our data set, Abl and Haspin, are illustrated in Figure 1C.

Inhibitor Resistance from Mutating Phe317^{Abl}

To determine the effects of mutations on kinase activity, we purified wild-type and mutant versions of our kinases from bacteria and subjected them to in vitro kinase assays with suitable substrates (Table 1). The effects on catalytic activity from individually mutating residues at the F317^{Abl} or G321^{Abl} positions varied significantly from kinase to kinase. For instance, mutations of F317^{Abl} to C, H, or Y (indicated as F317^{Abl}-X, where X is the amino acid substituent) left the catalytically activity essentially unaltered. Conversely mutations of G321^{Abl} to E, M, or V almost completely abrogated catalytic activity (Figure 2A; summarized in Figure S2).

Imatinib resistance of gatekeeper mutants of Abl (e.g., T315^{Abl}-I) can be overcome by using VX-680, originally described as an Aurora family inhibitor (Carter et al., 2005). In line with this idea, we found that VX-680 inhibits the imatinib-insensitive mutant T315^{Abl}-I to levels comparable to those of wild-type Abl (Figures 2B–2D). Remarkably, the F317^{Abl}-C and F317^{Abl}-H mutants were strongly resistant to VX-680, with a 15-fold increase of the half-maximal inhibitory concentration (Figure 2B). F317^{Abl}-H was also significantly resistant to imatinib, albeit to a lower degree compared with T315I (Figure 2D). We also tested our mutants against the second-generation Abl inhibitors dasatinib and nilotinib. F317^{Abl}-C and F317^{Abl}-H mutants were strongly resistant to dasatinib and nilotinib (Figures 2E and 2F). These observations suggest that at least one hinge loop mutant, F317^{Abl}-H, confers resistance to at least four unrelated inhibitors without grossly perturbing the catalytic activity of the mutated kinase.

An Inhibitor-Resistant Form of c-Src

We next asked whether these findings could be extended to other tyrosine kinases. The effects on inhibitor binding from mutating the gatekeeper residue of Src have been characterized (Blencke et al., 2004), but the effects from mutating Y340^{Src} and

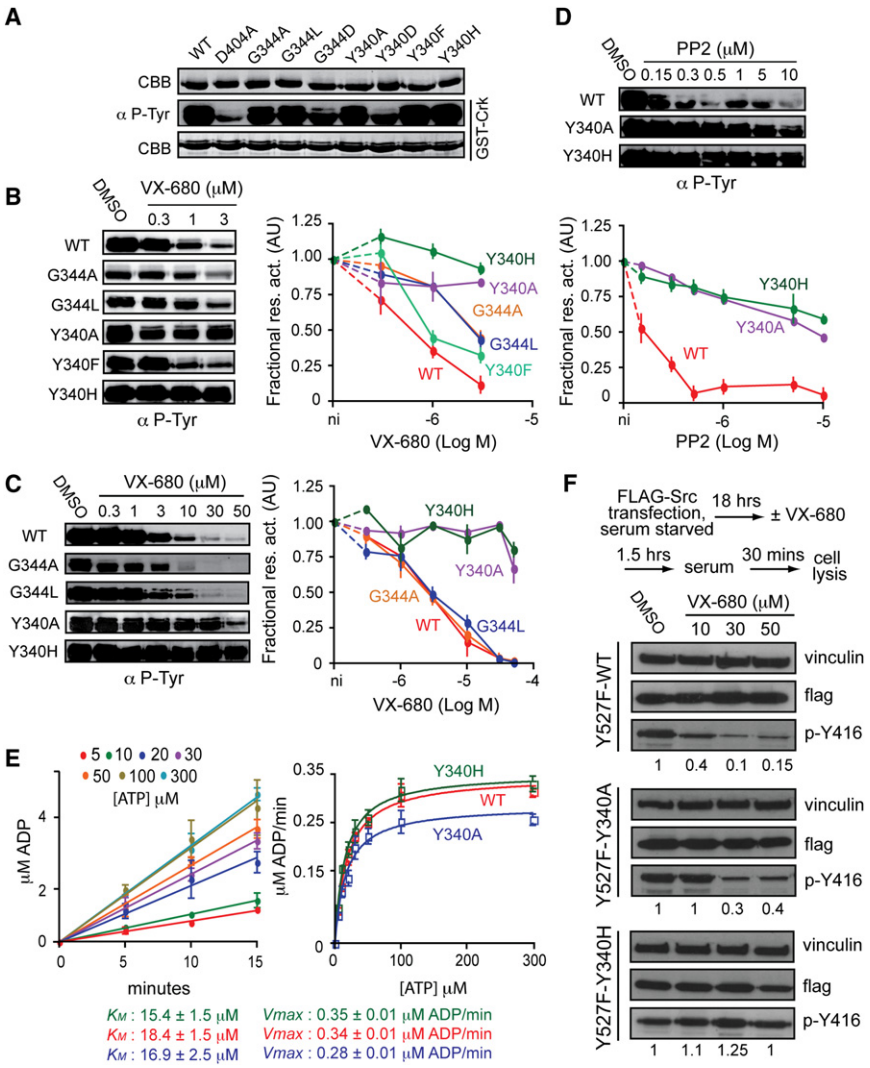

Figure 3. Cellular Resistance Formation of c-Src Tyrosine Kinase Mutants

(A) Activity test on wild-type c-Src and the indicated mutants.

(B–D) Wild-type Src and the indicated mutants were tested in the presence of increasing concentration of (B and C) VX-680 or (D) PP2. The DMSO solvent control (3% v/v) is indicated. Fractional residual activity (Fractional res. act.) from at least two independent experiments expressed as mean and standard deviation [arbitrary unit (AU)] was then quantified and plotted against the inhibitors concentration.

(E) c-Src ADP formation in presence of different concentration of ATP was monitored at different time points in a luminescence-based assay (left panel). The maximal velocity (V_{max}) obtained was plotted against different ATP concentrations to obtain the K_M value for the wild-type protein and inhibitor-resistant mutants (right panel). Each data point was collected in duplicate and kinetic parameters were obtained using GraphPad Prism v3.0 software.

(F) HeLa cells transiently expressing FLAG-Src-Y527F, Src-Y340H-Y527F, and Src-Y340A-Y527F were serum starved for 16 hr. Cells were treated with the indicated VX-680 concentrations for 90 min prior to serum stimulation and subsequent lysis. c-Src tyrosine kinase in total lysates was analyzed in parallel by immunoblotting with anti-pTyr416 Src family kinase-specific antibody, anti-flag antibody for transfection efficiency, and anti-vinculin loading control. Densitometric quantification was performed with ImageJ and the activity normalized against the transfection efficiency and with the loading control. Quantification of the residual activity is indicated below each lane of pTyr416. CBB = Coomassie brilliant blue; α P-Tyr = antibody recognizing phosphotyrosine residues.

G344^{Src}, equivalent to F317^{Abl} or G321^{Abl}, are unclear. We therefore mutated Y340^{Src} and G344^{Src} as indicated in Figure 3A. In contrast with c-Abl, substitution at G344^{Src} did not grossly affect the catalytic activity. Substitution Y340^{Src}-H or Y340^{Src}-A caused strong resistance toward VX-680 and PP2 (Hanke et al., 1996), with an approximately 80-fold increase in the half maximal inhibitory concentration (Figures 3B–3D). Importantly, neither mutation significantly affected the K_M for ATP, which was very similar to that of the wild-type kinase (Figure 3E).

We tested whether the mutations identified in vitro rescued the cellular activity of c-Src kinase in presence of a specific inhibitor. To activate c-Src tyrosine kinase, the carboxy-terminal Tyr527 residue, which negatively regulates c-Src upon C-terminal c-Src kinase (CSK)-mediated phosphorylation (Cooper and MacAuley, 1988), was mutated to phenylalanine. Mutants Y527F, Y340A-Y527F, and Y340H-Y527F of Src were transiently expressed in HeLa cells (Figure 3F) and c-Src kinase activity associated with each kinase was then measured by immunoblot analysis with an antiserum specifically recognizing c-Src-mediated autophosphorylation on its tyrosine residue 416 (Smart et al., 1981). VX-680 largely suppressed autophosphorylation of the constitutively active Y527F Src mutant. In contrast, the Src Y340H-Y527F double mutant revealed marked resistance even when the cells were treated with 50 μM VX-680 (Figure 4B). The Y340A-Y527F mutant showed milder levels of resistance than expected based on the in vitro experiments.

Substitutions of Glycine Render CK1δ, Phkγ, and Pak5 Resistant to Their Respective Chemical Inhibitors

Mutation of residues at the position equivalent to G321^{Abl} significantly affected the kinase activity of CK1δ and Pak5 (Figures 4A and 4G). The mutations, however, resulted in marked resistance to their cognate inhibitors (Figures 4B, 4C, 4H, and 4I). Specifically, the inhibitors D4476 and staurosporine (Rena et al., 2004; Tamaoki et al., 1986) were largely inert toward the G86^{CK1δ} and G529^{Pak5} mutants. D4476 inhibited wild-type CK1δ with a half-maximal concentration near 3 μM (Figures 4B and 4C), whereas the G86^{CK1δ}-D and G86^{CK1δ}-E mutants were essentially not inhibited at concentrations of D4476 as high as 30 μM. Similar effects were observed with the F525^{Pak5} and G529^{Pak5} mutants. For instance, the G529^{Pak5}-D mutant was largely insensitive to concentrations of staurosporine up to

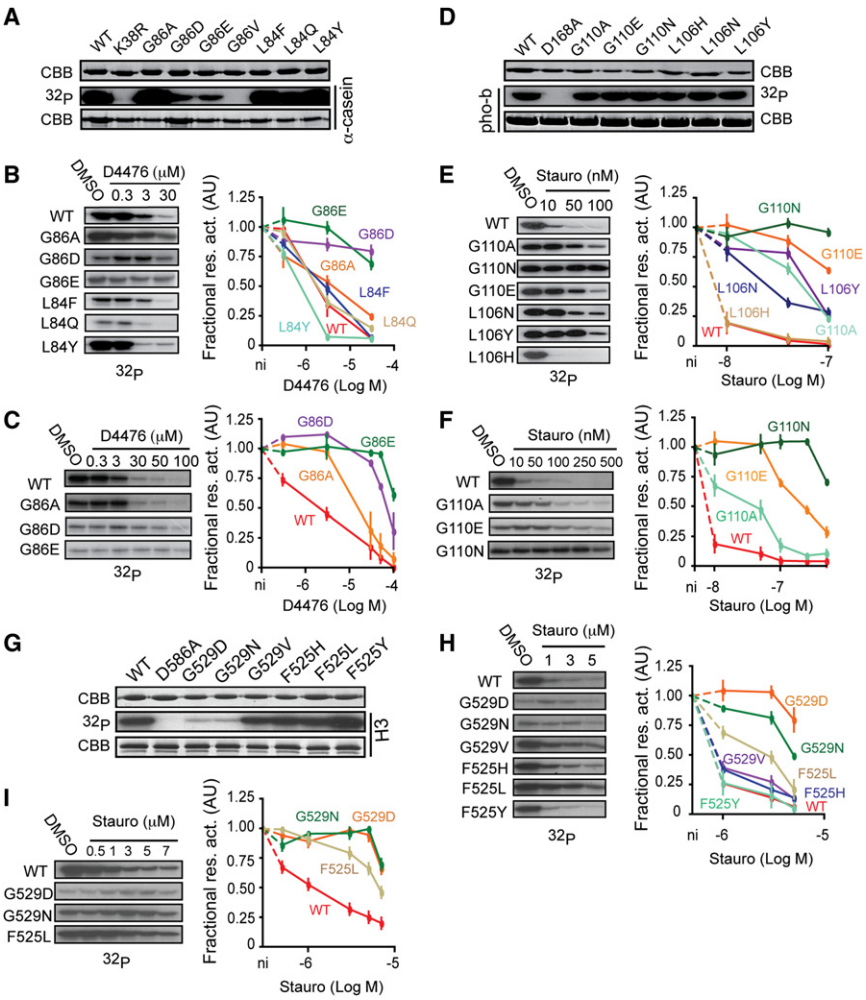

Figure 4. Inhibitor Resistance in CK1δ, Phkγ, and Pak5

(A) Activity test on wild-type human CK1δ.

(B and C) Wild-type CK1δ and the indicated mutants were tested in the presence of increasing concentration of D4476.

(D) Activity test on wild-type human CK1δ.

(E and F) Wild-type Phkγ and the indicated mutants were tested in the presence of increasing concentration of staurosporine.

(G) Activity test on wild-type human Pak5.

(H and I) Wild-type Pak5 and the indicated mutants were tested in the presence of increasing concentration of staurosporine. In all experiments, the DMSO solvent control (3% v/v) is also indicated. Fractional residual activity (Fractional res. act.) from at least two independent experiment expressed as mean and standard deviation [arbitrary unit (AU)] was then quantified and plotted against the inhibitors concentration. CBB, Coomassie brilliant blue; pho-b,phosphorylase b; Stauro,staurosporine; ^{32}p, autoradiography ^{32}P. See also Figure S3.

7 μM, and the G529^{Pak5}-N mutant was only slightly less effective and comparable to F525^{Pak5}-L (Figures 4H and 4I).

Phkγ appears to have a very stable scaffold, because all mutations we tested preserved its kinase activity (Figure 4D), and all of them, with the exception of L106^{Phkγ}-H, conferred variable levels of inhibitor resistance (Figures 4E and 4F). G110^{Phkγ}-N had the most penetrant effects, being completely resistant to staurosporine at all tested concentrations.

Analysis of the ''Phe'' mutants (i.e., in the position equivalent to Phe317 of Abl, see Figure 1B) in Phkγ and Pak5 (Figures 4E and 4H) suggested the possibility that mutations at this position might also have the potential to confer resistance to a generic kinase inhibitor such as staurosporine. To assess the generality of this idea, we extended the analysis to c-Abl and c-Src (Figure S3). Indeed, the F317^{Abl}-C and F317^{Abl}-H of Abl were strongly resistant to staurosporine, while Y340^{Src}-A and Y340^{Src}-H were moderately resistant to it.

Validating 5-Iodotubercidin as a Haspin Inhibitor

Haspin is an atypical kinase (Eswaran et al., 2009; Villa et al., 2009). Its kinase domain occupies the C-terminal part of the molecule. The large N-terminal region has unknown function (Higgins, 2003). It is a nuclear protein that associates with chromosomes to phosphorylate T3 of histone H3 (P-T3-H3) (Dai et al., 2005). This modification has been recently implicated in centromere recruitment of the Aurora B-containing chromosomal passenger complex at the centromere (Kelly et al., 2010; Wang et al., 2010; Yamagishi et al., 2010).

5-Iodotubercidin was initially reported to be a potent adenosine kinase inhibitor (Parkinson and Geiger, 1996). Recently, it was also identified as a potent in vitro inhibitor of Haspin (Eswaran et al., 2009). Because 5-iodotubercidin has not been yet fully characterized as a Haspin inhibitor, we set out to validate its potency in vitro and in vivo. In vitro, 5-iodotubercidin inhibited the isolated kinase domain of Haspin with an IC_{50} of 9 nM (Figure 5A). To determine the selectivity of inhibition, we set up an in vitro kinase assay with several human mitotic kinases, including Aurora A, Aurora B, Bub1, Cdk1:Cyclin B, Mps1, Nek2A, and Plk1. At 1 μM, 5-iodotubercidin failed to alter the activity of any of these kinases (Figure 5B).

We next sought to identify Haspin mutants that are insensitive to 5-iodotubercidin. Substitutions G609^{Haspin}-D, G609^{Haspin}-S, or G609^{Haspin}-V, while retaining a substantial fraction of kinase activity (Figure 5C), rendered Haspin resistant to high concentration of 5-iodotubercidin (Figures 5D and 5E). Conversely, substitution at F607^{Haspin} did not affect the susceptibility of Haspin to inhibition by 5-iodotubercidin. Decreased activity of the G609^{Haspin}-D or G609^{Haspin}-S mutants was not due to impaired ATP binding, because both mutants had a K_M for ATP that was similar to that of the wild-type kinase (Figure 5F). Thus, these mutants are likely affected in their ability to recognize their protein substrate.

To validate the effects of 5-iodotubercidin in cells, we first determined a working concentration of 5-iodotubercidin that

would inhibit Haspin activity, using the levels of P-T3-H3 as a read-out. As little as 0.5 μM 5-iodotubercidin efficiently inhibited histone H3 Thr3 phosporylation in HeLa cells, as assessed by indirect immunofluorescence with a specific antibody (Figure S4). This effect is consistent with those observed upon RNAi-mediated depletion of Haspin in mammalian cells (Dai et al., 2005).

Next, we created a Venus-Haspin fusion protein to express the wild-type and the $G609^{Haspin}$-D inhibitor-resistant mutant in HeLa cells (Nagai et al., 2002). After treatment with 5-iodotubercidin, cells were fixed and subjected to immunodecoration with antibodies recognizing P-T3-H3 (Figure 5G). At 5 μM 5-iodotubercidin, the P-T3-H3 signal observed upon transfection of the wild-type Venus-Haspin construct was largely abrogated. On the other hand, at 5 μM 5-iodotubercidin, the P-T3-H3 signal was largely preserved in cells expressing the $G609^{Haspin}$-D inhibitor-resistant mutant.

DISCUSSION

Inhibitor resistance in protein kinases is a scourge that limits the long-term clinical efficacy of small-molecule inhibitors. On the other hand, inhibitor resistance can be exploited as a tool for target identification and validation, and to evaluate the mechanism of action of new inhibitors. Here, we validate a general strategy to generate an inhibitor-resistant mutant without significant prior knowledge of their structural organization and without using cumbersome selection strategies. The strategy stems from previous observations that mutations at two defined positions in the hinge loop of Abl, Aurora B, and other kinases can confer resistance to active-site inhibitors. No systematic analysis of the generality of the effects of these mutations on inhibitor resistance has been carried out. Therefore, we set out to test the hypothesis that these positions can be targeted to develop a general strategy for inducing resistance toward active site inhibitors. We selected a diverse set of kinases and demonstrated that indeed the effects from mutating the hinge loop are very general and invariably result in inhibitor resistance. The generality of our findings is further reinforced by previous observations. Mutations at G216 in Aurora A, equivalent to $G160^{AurB}$, confer resistance to VX-680 (Scutt et al., 2009). Mutation of the structurally related G110 in p38α leads to marked resistance toward quinazolinone and pyridol-pyrimidine inhibitors (Fitzgerald et al., 2003). Furthermore, mutation of G95 in Plk4 leads to resistance toward VX-680 and MLN8054 (Sloane et al., 2010). Due to their generality, we are inclined to believe that our results might have significant clinical and technological applications.

A remarkable conclusion from our studies is that the catalytic activity of mutants at the two active-site positions we have identified is usually preserved, or only moderately reduced, although in some cases we also observed strong adverse effects on catalysis.

The mechanisms of inhibitor resistance in protein kinases are poorly understood. In many cases, resistance-conferring mutations affect residues that are distant from the active site. In these cases, the effects of mutation on resistance are usually difficult or impossible to rationalize. A class of mutations that received wide attention is that affecting the gatekeeper residue. In Abl, this mutation affects the potency of imatinib as an Abl inhibitor, but leaves the kinase susceptible to other inhibitors, such as VX680. The selectivity of the effects of gatekeeper mutants is due to the specific molecular structure of imatinib, a large inhibitor that penetrates deeply into the kinase's active site making extensive contacts with the gatekeeper. Larger gatekeeper residues create a problem of steric hindrance and prevent inhibitor binding. Binding of smaller inhibitors, such as VX-680, is unaffected, because the smaller inhibitors do not make contacts with the gatekeeper, implying that this residue does not act as a selectivity filter for the smaller inhibitor. The hinge loop residues discussed here, on the other hand, are implicated as selectivity filters of essentially any active-site ATP-competitive inhibitor, which is why their mutation invariably results in resistance, regardless of the type of active-site inhibitor used. These results predict that the previously described hinge loop mutants of Abl will be resistant not only to imatinib, but to essentially any alternative ATP site inhibitors of the Abl kinase, providing a strong argument toward alternative curative strategies for patients that relapse with such mutations.

SIGNIFICANCE

Protein kinases are considered ideal targets for chemical inhibition. Several classes of small-molecule kinase inhibitors are available, and several kinase inhibitors are being tested in clinical trials, most often as anticancer inhibitors (Knight and Shokat, 2005). Inhibitor resistance arises due to mutations in the kinase scaffold, or, in case of multidomain kinases, also in adjacent domains (Daub et al., 2004). Here, we have shown that mutations at either of two specific positions in the active site of protein kinases usually results in inhibitor resistance with relatively mild effects on kinase activity. We demonstrate that this strategy can lead to the isolation of inhibitor-resistant mutants of a kinase of choice without significant prior knowledge of the structural basis of the kinase-inhibitor pair, except that the inhibitor is a nonallosteric, ATP-competitive inhibitor. We also show that mutation of the "Phe" residue within the hinge loop usually renders the affected kinases insensitive to the unspecific kinase inhibitor staurosporine. This strategy might become extremely useful for the validation of new inhibitors. For instance, we validate Haspin as a target of 5-iodotubercidin, a compound that was previously shown to bind to Haspin (Eswaran et al., 2009), but whose ability to target Haspin in living cells had not been characterized. Furthermore, the strategy might be a useful aid in the characterization of specific phenotypes. The approach discussed here is complementary to a widely used approach based on the substitution of the gatekeeper residue with smaller residues, which promotes the sensitization of the mutant kinase to specific inhibitors (Bishop et al., 2001). Thus, the approach discussed here has the potential to become widely applicable in kinase target validation in vitro and in live cells and organisms.

EXPERIMENTAL PROCEDURES

Cell Culture, Transfection, and Synchronization

HeLa cells were grown in DME (EuroClone) supplemented with 10% fetal bovine serum (HyClone) and 2 mM L-glutamine. FuGENE 6 (Roche Applied

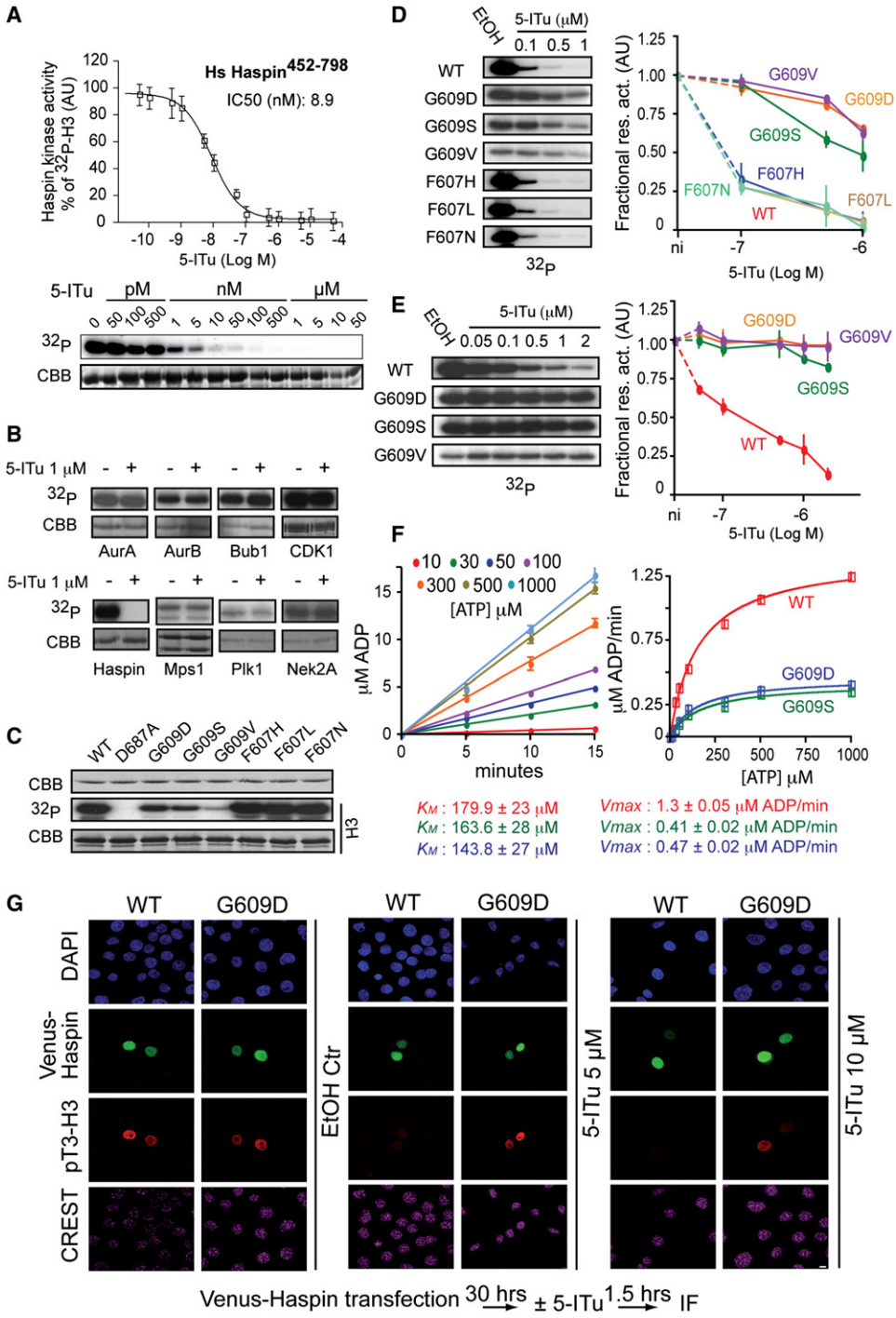

Figure 5. 5-Iodotubercidin Is a Potent Haspin Inhibitor

(A) A kinase assay on the kinase domain of human Haspin with the indicated concentrations of 5-iodotubecidin (5-ITu). The substrate is histone H3.

(B) The indicated recombinant, purified mitotic kinases were tested with the appropriated substrates for their sensitivity to 1 µM 5-ITu. Error bars are mean ± SEM.

(C) The activity of wild-type Haspin and of selected mutants.

(D and E) The activity of wild-type and indicated Haspin mutants was tested in presence of increasing concentration of 5-ITu. The ethanol (EtOH) solvent control (3% v/v) is indicated. Fractional residual activity (Fractional res. act.) from at least two independent experiment expressed as mean and standard deviation [arbitrary unit (AU)] was then quantified and plotted against the inhibitors concentration.

(F) Haspin wild-type ADP formation in presence of different concentration of ATP was monitored at different time points in a luminescence assay (left panel). The V_{max} obtained were then plotted against different ATP concentrations to obtain the K_M value for the wild-type protein and inhibitor-resistant mutants (right panel).

Sciences) was used for transfection of HeLa cells following the manufacturer's suggestions. Nocodazole (3.3 μM) and thymidine (2 mM) were obtained from Sigma-Aldrich. MG132 (EMD) was used at 10 μM.

Antibodies for Immunoblotting, Kinase Substrates, and Inhibitors

The following antibodies were used for immunoblotting: mouse anti-phosphoTyr (working dilution 1:2000; Upstate), rabbit anti-phosphoTyr416 c-Src (working dilution 1:2000; Cell Signaling), mouse anti-flag (working dilution 1:8000; Sigma), rabbit anti-vinculin (working dilution 1:10000; Sigma). Phosphorylase b and α-casein were from Sigma. Histone H3 was from Roche. 5-Iodotubercidin was from Cayman Chemical. PP2, D4476, and staurosporine were from Calbiochem, VX-680 and imatinib from LC Laboratories, and dasatinib and nilotinib from Santa Cruz Biotechnology, Inc.

Plasmids

A segment of a human cDNA encoding CK1δ$^{1-303}$ was subcloned with BamHI-XhoI sites of a pGEX-6P vector (GE Healthcare) as a C-terminal fusion to GST, with an intervening PreScission protease site. Vectors carrying cDNA encoding Phkγ$^{2-297}$, Pak5$^{425-715}$, and Crk$^{120-225}$ were obtained respectively from the University of Dundee (UK), University of Oxford (UK), and the IFOM institute (IT). Expression plasmid carrying Haspin$^{452-798}$ was described previously (Villa et al., 2009). A segment of mouse cDNA encoding c-Abl$^{229-511}$ and chicken c-Src$^{251-533}$ were subcloned with BamHI-HindIII sites in a pGEX-6P vector. The cDNA of the tyrosin phosphatase from *yersinia pestis* YopH was cloned into a pACYC-Duet (Novagen) with NcoI-XhoI sites. For mammalian expression the full-length sequence of chicken c-Src$^{1-533}$ has been subcloned with BamHI-XhoI sites into a pcDNA3.1 (Invitrogen) as a C terminus fusion of a flag peptide. Haspin$^{1-798}$ has been subcloned with EcoRV-NotI sites into a pcDNA5-FRT/TO (Invitrogen) as a C terminus fusion of the fluorescent protein Venus (Nagai et al., 2002). Point mutants were created with the QuikChange kit (Stratagene) according to the manufacturer's suggestions. All constructs were sequence verified.

Protein Expression for Kinetic Analysis

GST fusion vectors of Crk$^{120-225}$, Haspin$^{452-798}$, Pak5$^{251-533}$, CK1δ$^{1-303}$, Phkγ$^{2-297}$ and indicated mutants were used to transform BL21 *Escherichia coli* strain. All wild-type and mutated versions were expressed and purified identically. Expression was induced with 0.25 mM IPTG at OD600 = 0.7–0.9 and protracted for 12–16 hr at 23°C. Bacterial cells were harvested by centrifugation at 4000 × g for 15 min in a Beckman JLA 8.1 rotor, and the pellets were resuspended in lysis buffer (50 mM Tris HCl [pH 7.6], 400 mM NaCl, 1 mM DTT, 1 mM EDTA, 5% glycerol, Roche Complete Protease Inhibitor Cocktail Tablets). Cells were lysed by sonication, and lysates were cleared by centrifugation at 23,000 × g for 45–60 min on a JA25-50 rotor. The supernatants were incubated with 300 μl of GST Sepharose Fast Flow (Amersham Biosciences) per liter of bacterial culture previously washed with PBS and equilibrated with lysis buffer. After 2 hr at 4°C, beads were washed with 30 volumes of lysis buffer and equilibrated in cleavage buffer (50 mM Tris [pH 7.6], 300 mM NaCl, 5% glycerol, 1 mM DTT, 1 mM EDTA). All the fusion proteins were subjected to GST cleavage with the exception GST-Crk$^{120-225}$ that was eluted with 20 mM reduced glutathione. For GST cleavage, 10 units of PreScission Protease (Amersham Biosciences) per milligram of substrate was added, and the incubation was protracted for 16 hr at 4°C. The purified kinases containing fractions were collected and employed for subsequent enzymatic analysis. c-Abl$^{229-511}$ and c-Src$^{251-533}$ were cotransformed with a plasmid encoding for the *Yersinia pestis* YopH tyrosine phosphatase to limit the toxicity of the kinases catalytic activity (Seeliger et al., 2005). GST purification of c-Abl and c-Src was then performed as previously described.

Radioactive Kinase Assays

All assays (30 μl volume) were performed at room temperature (25°C) for 60 min, quenched with SDS loading buffer, and resolved on 14% SDS-PAGE. Incorporation of ^{32}P was visualized by autoradiography. Densitometry analysis was performed using ImageJ software (National Institutes of Health). IC_{50} values were calculated from log-dose response curves using Prism 4 software (GraphPad Software, Inc.). Reactions for CK1δ were carried out in a solution containing 20 mM HEPES [pH 7.5], 10 mM $MgCl_2$, 0.1 mM EDTA. Final substrate concentrations in the assay were 20 μM ATP (5 μCi γ-^{32}P-ATP), 5 μM of α-casein, and 5 nM kinase. Reactions for Phkγ were carried out in a solution containing 50 mM Tris [pH 8.6], 10 mM $MgCl_2$, 0.04 mM $CaCl_2$. Final substrate concentrations in the assay were 50 μM ATP (5 μCi γ-^{32}P-ATP), 15 μM of phosphorylase b, and 50 nM kinase. Reactions for Haspin were carried out in a solution containing 25 mM Tris [pH 7.5], 10 mM $MgCl_2$, 150 mM NaCl. Final substrate concentrations in the assay were 250 μM ATP (5 μCi γ-^{32}P-ATP), 5 μM of histone H3, and 5 nM kinase. Reactions for Pak5 were carried out in a solution containing 25 mM Tris [pH 7.5], 10 mM $MgCl_2$, 150 mM NaCl. Final substrate concentrations in the assay were 50 μM ATP (5 μCi γ-^{32}P-ATP), 5 μM of histone H3, and 50 nM kinase. Inhibitors were tested for their ability to inhibit candidate's kinases activity in vitro. Indicated amounts of inhibitors were added to the reaction and DMSO was used as control. To test 5-iodotubercidin specificity, mitotic kinases were purified and assayed as described elsewhere (Santaguida et al., 2010).

Kinase Assays Employing pTyr-Specific Antibodies

Reactions for c-Src and c-Abl kinases were carried out in a solution containing 100 mM Tris [pH 8.0] and 10 mM $MgCl_2$. Final substrate concentrations in the assay were 50 μM ATP, 10 μM of GST-Crk1, and 50 nM kinase. Reaction were initiated by the addition of ATP and $MgCl_2$ and carried out at 30°C for 30 min and finally terminated by adding SDS-page loading buffer. Inhibition assay reactions were then separated on a 15% SDS-PAGE gel and transferred onto a nitrocellulose membrane. The membrane was blocked in 50 mM Tris-HCl [pH 7.5], 150 mM NaCl, 0.1% (v/v) Tween (TBS-Tween), and 5% (w/v) BSA for 1 hr. The membrane was then incubated with the same buffer for 16 hr at 4°C in the presence of monoclonal antibody directed against epitope phospho-Tyr. Detection was performed using horseradish peroxidase-conjugated secondary antibody and the enhanced chemiluminescence (ECL Amersham Pharmacia Biotech) reagent.

ADP Luminescent Assay

Kinetic analyses of Haspin$^{452-798}$ and c-Src$^{221-533}$ and the indicated mutants were performed using a luminometric kinase assay varying the concentration of ATP using the ADP-Glo reagents (Promega). Haspin kinase (5 nM) was assayed in a reaction (10 μl) containing 25 mM Tris (pH 7.6), 10 mM $MgCl_2$, 150 mM NaCl, 1 mM EDTA, 1 mM DTT, varied concentrations of ATP, and 5 μM of histone H3 (Roche) and followed for 15 min. c-Src kinase (50 nM) was assayed in a reaction (10 μl) containing 100 mM Tris (pH 8), 10 mM $MgCl_2$, varied concentrations of ATP, and 10 μM of GST-Crk1 and followed for 15 min. The overall rate of reaction is determined as the slope of the decreasing phase of the reaction. Each data point was collected in duplicate and kinetic parameters were obtained using GraphPad Prism v3.0 software.

Immunofluorescence Microscopy

HeLa cells were transfected with indicated Venus-Haspin constructs using the Fugene transfection reagent according to the manufacturer's instructions. The inhibitor, or the equivalent volume of ethanol as a control, was added to the tissue culture medium for 90 min and the cells were fixed using 4% PFA in PBS. The following antibodies were used: anticentromeric antibody (working dilution 1:100; Antibodies Inc.) rabbit anti-histone H3 (working dilution 1:50; Cell signaling). Cy3- and Cy5-labeled and Alexa Fluor 488-labeled secondary antibodies for immunofluorescence were purchased from Jackson ImmunoResearch Laboratories, Inc. and Invitrogen, respectively. DNA was stained with DAPI. The coverslips were mounted using Mowiol mounting media. Cells were imaged using a confocal microscope (TCS SP2; Leica) equipped with a 63 × NA 1.4 objective lens using the LCS 3D software (Leica).

(G) Transiently transfected HeLa cells expressing Venus-Haspin wild-type and the 5-ITu-resistant mutant G609D were treated with the indicated 5-ITu concentrations for 90 min. Immunofluorescence images demonstrated that expression of Venus-HaspinG609D conferred inhibitor resistance to the transfected cells, which retain the phospho-Thr3 signal in the presence of the inhibitor. CBB,Coomassie brilliant blue; ^{32}p, autoradiography ^{32}P. Scale bar represents 5 μm. See also Figure S4.

Images were imported in Photoshop CS3 (Adobe Systems, Inc.), and levels were adjusted.

Cell Stimulation, Inhibitor Treatment, and Cell Lysis

HeLa cells were transfected with indicated flag-SrcY527F plasmid using the Fugene transfection reagent according to the manufacturer's suggestions. The cells transfected with indicated flag-SrcY527F constructs were deprived of serum for 18 hr. The inhibitor, or the equivalent volume of DMSO as a control, was added to the tissue culture medium 90 min prior to stimulation. The cells were then stimulated with serum for 30 min. HeLa cells were finally harvested by trypsinization and lysed in 50 mM HEPES (pH 7.5), 150 mM NaCl, 0.5% NP40, 1% glycerol, 5 mM EDTA, 10 mM Na_3VO_4, 50 mM NaF, 20 mM Na_4-pyrophosphate, and protease inhibitor cocktail (Calbiochem) for 20 min on ice. Cell lysates were centrifuged for 15 min at 13,000 rpm at 4°C in an Eppendorf microcentrifuge. Protein amounts were measured with protein assay reagent (Bio-Rad Laboratories) as specified by the manufacturer, and equivalent amounts of total protein of each cell lysate were analyzed by western blotting. Densitometry analysis was performed using ImageJ software (National Institutes of Health).

SUPPLEMENTAL INFORMATION

Supplemental Information includes four figures and can be found with this article online at doi:10.1016/j.chembiol.2011.04.013.

ACKNOWLEDGMENTS

We thank the members of the Musacchio laboratory for many helpful discussions and D. R. Alessi, S. Knapp, E. Maspero, G. Scita, and Z. Y. Zhang for sharing reagents. The work was funded by the Association for International Cancer Research and the Italian Association for Cancer Research. S.S. is supported by a fellowship from the Italian Foundation for Cancer Research. F.V. is a former EMBO long-term postdoctoral fellow.

Received: January 16, 2011
Revised: April 10, 2011
Accepted: April 26, 2011
Published: August 25, 2011

REFERENCES

Aguilera, D.G., and Tsimberidou, A.M. (2009). Dasatinib in chronic myeloid leukemia: a review. Ther. Clin. Risk Manag. *5*, 281–289.

Bikker, J.A., Brooijmans, N., Wissner, A., and Mansour, T.S. (2009). Kinase domain mutations in cancer: implications for small molecule drug design strategies. J. Med. Chem. *52*, 1493–1509.

Bishop, A.C., Buzko, O., and Shokat, K.M. (2001). Magic bullets for protein kinases. Trends Cell Biol. *11*, 167–172.

Blencke, S., Zech, B., Engkvist, O., Greff, Z., Orfi, L., Horvath, Z., Keri, G., Ullrich, A., and Daub, H. (2004). Characterization of a conserved structural determinant controlling protein kinase sensitivity to selective inhibitors. Chem. Biol. *11*, 691–701.

Branford, S., Rudzki, Z., Walsh, S., Grigg, A., Arthur, C., Taylor, K., Herrmann, R., Lynch, K.P., and Hughes, T.P. (2002). High frequency of point mutations clustered within the adenosine triphosphate-binding region of BCR/ABL in patients with chronic myeloid leukemia or Ph-positive acute lymphoblastic leukemia who develop imatinib (STI571) resistance. Blood *99*, 3472–3475.

Capdeville, R., Buchdunger, E., Zimmermann, J., and Matter, A. (2002). Glivec (STI571, imatinib), a rationally developed, targeted anticancer drug. Nat. Rev. Drug Discov. *1*, 493–502.

Carter, T.A., Wodicka, L.M., Shah, N.P., Velasco, A.M., Fabian, M.A., Treiber, D.K., Milanov, Z.V., Atteridge, C.E., Biggs, W.H., 3rd, Edeen, P.T., et al. (2005). Inhibition of drug-resistant mutants of ABL, KIT, and EGF receptor kinases. Proc. Natl. Acad. Sci. USA *102*, 11011–11016.

Choi, Y.L., Soda, M., Yamashita, Y., Ueno, T., Takashima, J., Nakajima, T., Yatabe, Y., Takeuchi, K., Hamada, T., Haruta, H., et al. (2010). EML4-ALK mutations in lung cancer that confer resistance to ALK inhibitors. N. Engl. J. Med. *363*, 1734–1739.

Cohen, P. (2002). Protein kinases: the major drug targets of the twenty-first century? Nat. Rev. Drug Discov. *1*, 309–315.

Cooper, J.A., and MacAuley, A. (1988). Potential positive and negative autoregulation of p60c-src by intermolecular autophosphorylation. Proc. Natl. Acad. Sci. USA *85*, 4232–4236.

Dai, J., Sultan, S., Taylor, S.S., and Higgins, J.M. (2005). The kinase haspin is required for mitotic histone H3 Thr 3 phosphorylation and normal metaphase chromosome alignment. Genes Dev. *19*, 472–488.

Daub, H., Specht, K., and Ullrich, A. (2004). Strategies to overcome resistance to targeted protein kinase inhibitors. Nat. Rev. Drug Discov. *3*, 1001–1010.

Eswaran, J., Patnaik, D., Filippakopoulos, P., Wang, F., Stein, R.L., Murray, J.W., Higgins, J.M., and Knapp, S. (2009). Structure and functional characterization of the atypical human kinase haspin. Proc. Natl. Acad. Sci. USA *106*, 20198–20203.

Fitzgerald, C.E., Patel, S.B., Becker, J.W., Cameron, P.M., Zaller, D., Pikounis, V.B., O'Keefe, S.J., and Scapin, G. (2003). Structural basis for p38alpha MAP kinase quinazolinone and pyridol-pyrimidine inhibitor specificity. Nat. Struct. Biol. *10*, 764–769.

Girdler, F., Sessa, F., Patercoli, S., Villa, F., Musacchio, A., and Taylor, S. (2008). Molecular basis of drug resistance in aurora kinases. Chem. Biol. *15*, 552–562.

Gorre, M.E., Mohammed, M., Ellwood, K., Hsu, N., Paquette, R., Rao, P.N., and Sawyers, C.L. (2001). Clinical resistance to STI-571 cancer therapy caused by BCR-ABL gene mutation or amplification. Science *293*, 876–880.

Hanke, J.H., Gardner, J.P., Dow, R.L., Changelian, P.S., Brissette, W.H., Weringer, E.J., Pollok, B.A., and Connelly, P.A. (1996). Discovery of a novel, potent, and Src family-selective tyrosine kinase inhibitor. Study of Lck- and FynT-dependent T cell activation. J. Biol. Chem. *271*, 695–701.

Higgins, J.M. (2003). Structure, function and evolution of haspin and haspin-related proteins, a distinctive group of eukaryotic protein kinases. Cell. Mol. Life Sci. *60*, 446–462.

Hung, C.H., Thomas, L., Ruby, C.E., Atkins, K.M., Morris, N.P., Knight, Z.A., Scholz, I., Barklis, E., Weinberg, A.D., Shokat, K.M., et al. (2007). HIV-1 Nef assembles a Src family kinase-ZAP-70/Syk-PI3K cascade to downregulate cell-surface MHC-I. Cell Host Microbe *1*, 121–133.

Karaman, M.W., Herrgard, S., Treiber, D.K., Gallant, P., Atteridge, C.E., Campbell, B.T., Chan, K.W., Ciceri, P., Davis, M.I., Edeen, P.T., et al. (2008). A quantitative analysis of kinase inhibitor selectivity. Nat. Biotechnol. *26*, 127–132.

Kelly, A.E., Ghenoiu, C., Xue, J.Z., Zierhut, C., Kimura, H., and Funabiki, H. (2010). Survivin reads phosphorylated histone H3 threonine 3 to activate the mitotic kinase Aurora B. Science *330*, 235–239.

Knight, Z.A., and Shokat, K.M. (2005). Features of selective kinase inhibitors. Chem. Biol. *12*, 621–637.

Kobayashi, S., Boggon, T.J., Dayaram, T., Janne, P.A., Kocher, O., Meyerson, M., Johnson, B.E., Eck, M.J., Tenen, D.G., and Halmos, B. (2005). EGFR mutation and resistance of non-small-cell lung cancer to gefitinib. N. Engl. J. Med. *352*, 786–792.

Krishnamurty, R., and Maly, D.J. (2010). Biochemical mechanisms of resistance to small-molecule protein kinase inhibitors. ACS Chem. Biol. *5*, 121–138.

Liu, Y., and Gray, N.S. (2006). Rational design of inhibitors that bind to inactive kinase conformations. Nat. Chem. Biol. *2*, 358–364.

Manning, G., Whyte, D.B., Martinez, R., Hunter, T., and Sudarsanam, S. (2002). The protein kinase complement of the human genome. Science *298*, 1912–1934.

Melo, J.V., and Chuah, C. (2007). Resistance to imatinib mesylate in chronic myeloid leukaemia. Cancer Lett. *249*, 121–132.

Nagai, T., Ibata, K., Park, E.S., Kubota, M., Mikoshiba, K., and Miyawaki, A. (2002). A variant of yellow fluorescent protein with fast and efficient maturation for cell-biological applications. Nat. Biotechnol. *20*, 87–90.

Okram, B., Nagle, A., Adrian, F.J., Lee, C., Ren, P., Wang, X., Sim, T., Xie, Y., Xia, G., Spraggon, G., et al. (2006). A general strategy for creating "inactive-conformation" abl inhibitors. Chem. Biol. *13*, 779–786.

Pao, W., Miller, V.A., Politi, K.A., Riely, G.J., Somwar, R., Zakowski, M.F., Kris, M.G., and Varmus, H. (2005). Acquired resistance of lung adenocarcinomas to gefitinib or erlotinib is associated with a second mutation in the EGFR kinase domain. PLoS Med. *2*, e73.

Parkinson, F.E., and Geiger, J.D. (1996). Effects of iodotubercidin on adenosine kinase activity and nucleoside transport in DDT1 MF-2 smooth muscle cells. J. Pharmacol. Exp. Ther. *277*, 1397–1401.

Rena, G., Bain, J., Elliott, M., and Cohen, P. (2004). D4476, a cell-permeant inhibitor of CK1, suppresses the site-specific phosphorylation and nuclear exclusion of FOXO1a. EMBO Rep. *5*, 60–65.

Santaguida, S., Tighe, A., D'Alise, A.M., Taylor, S.S., and Musacchio, A. (2010). Dissecting the role of MPS1 in chromosome biorientation and the spindle checkpoint through the small molecule inhibitor reversine. J. Cell Biol. *190*, 73–87.

Schindler, T., Bornmann, W., Pellicena, P., Miller, W.T., Clarkson, B., and Kuriyan, J. (2000). Structural mechanism for STI-571 inhibition of abelson tyrosine kinase. Science *289*, 1938–1942.

Scutt, P.J., Chu, M.L., Sloane, D.A., Cherry, M., Bignell, C.R., Williams, D.H., and Eyers, P.A. (2009). Discovery and exploitation of inhibitor-resistant aurora and polo kinase mutants for the analysis of mitotic networks. J. Biol. Chem. *284*, 15880–15893.

Seeliger, M.A., Young, M., Henderson, M.N., Pellicena, P., King, D.S., Falick, A.M., and Kuriyan, J. (2005). High yield bacterial expression of active c-Abl and c-Src tyrosine kinases. Protein Sci. *14*, 3135–3139.

Shah, N.P., Tran, C., Lee, F.Y., Chen, P., Norris, D., and Sawyers, C.L. (2004). Overriding imatinib resistance with a novel ABL kinase inhibitor. Science *305*, 399–401.

Sloane, D.A., Trikic, M.Z., Chu, M.L., Lamers, M.B., Mason, C.S., Mueller, I., Savory, W.J., Williams, D.H., and Eyers, P.A. (2010). Drug-resistant aurora A mutants for cellular target validation of the small molecule kinase inhibitors MLN8054 and MLN8237. ACS Chem. Biol. *5*, 563–576.

Smart, J.E., Oppermann, H., Czernilofsky, A.P., Purchio, A.F., Erikson, R.L., and Bishop, J.M. (1981). Characterization of sites for tyrosine phosphorylation in the transforming protein of Rous sarcoma virus (pp60v-src) and its normal cellular homologue (pp60c-src). Proc. Natl. Acad. Sci. USA *78*, 6013–6017.

Soverini, S., Martinelli, G., Colarossi, S., Gnani, A., Castagnetti, F., Rosti, G., Bosi, C., Paolini, S., Rondoni, M., Piccaluga, P.P., et al. (2006). Presence or the emergence of a F317L BCR-ABL mutation may be associated with resistance to dasatinib in Philadelphia chromosome-positive leukemia. J. Clin. Oncol. *24*, e51–e52.

Suryanarayan, K., Hunger, S.P., Kohler, S., Carroll, A.J., Crist, W., Link, M.P., and Cleary, M.L. (1991). Consistent involvement of the bcr gene by 9;22 breakpoints in pediatric acute leukemias. Blood *77*, 324–330.

Tamaoki, T., Nomoto, H., Takahashi, I., Kato, Y., Morimoto, M., and Tomita, F. (1986). Staurosporine, a potent inhibitor of phospholipid/Ca++dependent protein kinase. Biochem. Biophys. Res. Commun. *135*, 397–402.

Villa, F., Capasso, P., Tortorici, M., Forneris, F., de Marco, A., Mattevi, A., and Musacchio, A. (2009). Crystal structure of the catalytic domain of Haspin, an atypical kinase implicated in chromatin organization. Proc. Natl. Acad. Sci. USA *106*, 20204–20209.

Wang, F., Dai, J., Daum, J.R., Niedzialkowska, E., Banerjee, B., Stukenberg, P.T., Gorbsky, G.J., and Higgins, J.M. (2010). Histone *H3*, Thr-3.

Wong, S., and Witte, O.N. (2004). The BCR-ABL story: bench to bedside and back. Annu. Rev. Immunol. *22*, 247–306.

Yamagishi, Y., Honda, T., Tanno, Y., and Watanabe, Y. (2010). Two histone marks establish the inner centromere and chromosome bi-orientation. Science *330*, 239–243.

Zhang, J., Yang, P.L., and Gray, N.S. (2009). Targeting cancer with small molecule kinase inhibitors. Nat. Rev. Cancer *9*, 28–39.

